GSA Data Repository 2019253

Camp, V.E., 2019, Plume-modified mantle flow in the northern Basin and Range and southern Cascadia back-arc region since ca. 12 Ma: Geology, https://doi.org/10.1130/G46144.1

Summary of Flow Mantle-Models and an Approximation of Yellowstone Plume Volume Flux and Mantle Flow Rate

The following is available online at http://www.geosociety.org/datarepository/2019/, or on request from editing@geosociety.org: (1) Summary of mantle-flow models and comparative seismic data, including Figures DR1 (modeling results of Lowry et al., 2000) and Figure DR2 (cross-sections of the regional low-velocity upper-mantle feature of Wagner et al. (2010) and James et al. (2011), and (2) Approximation of Yellowstone plume volume flux for source melting and mantle flow rate, including Figure DR3 (diagrammatic representation of plume tail melting).

1. Summary of Relevant Mantle-Flow Models for the Yellowstone Hotspot and Comparative Data from Seismic Tomography.

The recent model simulations of Leonard and Liu (2016) and Zhou et al. (2018) describe a putative Yellowstone plume that is incapable of producing the voluminous magmatism associated with the Columbia River Basalt Province and the Yellowstone-Snake River Plain (YSRP). Instead, Zhou et al. (2018) attribute flood-basalt volcanism and the eastward migration of volcanism along the YSRP to the eastward flow of shallow mantle, in the opposite direction of plate motion, driven by a sinking Farallon slab beneath central-eastern United States. Such models that invoke a shallow-mantle genesis for volcanism along the YSRP cannot readily explain the recent tomographic evidence of Nelson and Grand (2018) for a Yellowstone plume source that descends to the core-mantle boundary, and they also have difficulty explaining trace-element and isotopic data consistent with such a lower-mantle source (e.g., Wolff et al., 2013). The relatively high $^{3}He/^{4}He$ ratios for Columbia River basalt and YSRP basalt, for example, are typically considered to be robust indicators of a deep mantle origin (Dodson et al., 1997; Graham et al., 2009). Zhou et al. (2018) note that these high $^{3}He/^{4}He$ ratios could be explained by a more dynamic Yellowstone plume if their model simulations were to include a more realistic rheology involving deep-mantle materials, but they still maintain their preference for an inconsequential Yellowstone plume. These model simulations for a shallow-mantle hotspot are innovative, consistent with model constraints, and significant in providing a platform for future studies on mantle dynamics;

however, they also require one to accept that the current location of the Yellowstone plume directly underlying the hotspot today is mere coincidence.

The models of Leonard and Liu (2016) and Zhou et al. (2018) are largely focused on subducting slabs as the major control on upper-mantle flow. Lowry et al. (2000) provided an earlier and different approach focused on synthesizing topography, gravity, seismic refraction velocity, and surface heat flow data sets which they used to determine the dynamic elevation of the U.S. Cordillera; i.e., the topography derived from buoyancy variations beneath the lithosphere. They determined that the largest of the dynamic elevation anomalies (up to 2 km over a diameter of ~1000 km) incorporates the YSRP and northern Basin and Range, consistent with the earlier findings of Parsons et al. (1994) and Saltus and Thompson (1995).

This large dynamic elevation anomaly defines the Yellowstone hotspot swell, which is similar to oceanic hotspot swells that also display (1) symmetry about a hotspot track, (2) a ~1000 km cross-sectional width, (3) elongation in the direction of plate motion, and (4) decreasing elevation downstream of the hotspot location (e.g., Crough, 1983; Ribe and Christensen, 1994; Wolfe et al., 2009). These characteristics are predicted in mantle-flow models, but they are also observed in mantle tomographic studies where buoyant hot plume material is sheared by the motion of a viscous overlying plate (e.g., Ribe and Christensen, 1994, 1999; Sleep, 1996; Wolfe et al., 2009). The 3-D numerical model of Lowry et al. (2000) adequately explains the dynamic uplift of the Yellowstone swell (Fig. DR1), and it is consistent with plume rise and distortion of plume-modified mantle in the direction of plate motion, as is also observed beneath Hawaii and elsewhere (e.g., Wolfe et al., 2009).

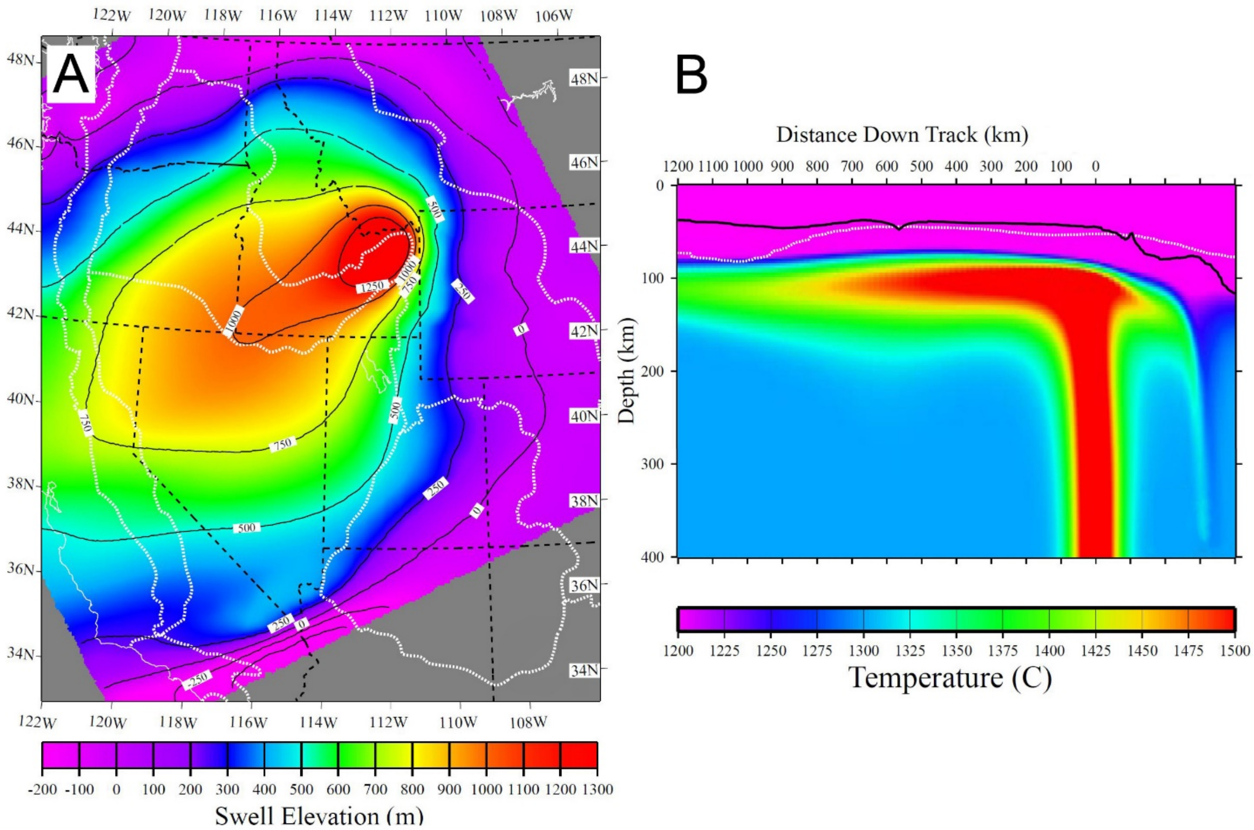

Figure DR1. Modeling results of Lowry et al. (2000). A. Numerical model of Yellowstone swell elevation for variable thickness lithosphere (determined by depth to 10^{21} Pa s viscosity) and 3 x 10^{-16} s^{-1} uniaxial extension southwest of the Yellowstone plume (from Lowry et al., 2000). B. Cross-section of temperature field along the track of the hotspot in the direction of plate motion (from Lowry et al., 2000). White line is 1000 ^{o}C isotherm derived from surface heatflow; black line is depth to the 10^{21} Pa s isopoise surface.

The model of Lowry et al. (2000) defines a thermal mantle structure for the Yellowstone hotspot (Fig. DR1B) that is remarkably similar to the regional layer of low-density mantle beneath southern Oregon, northern Nevada and southern Idaho, as resolved in a variety of seismic studies (e.g., Obrebski et al., 2010; Wagner et al., 2010; Long et al., 2012; James et al., 2011, Tian and Zhou, 2012). Seismic cross-sections across this low-density mantle are illustrated, for example, in Figure DR2 modified from James et al. (2011) and Wagner et al. (2010). The modeled feature (Fig. DR1B) and the seismically defined feature (Fig. DR2) are similar in depth, dimensions, orientation, and decreasing thermal intensity downstream to the southwest. Both the modeled and seismically defined features bend downward beneath Yellowstone into the plume conduit that connects the feature to a lower mantle source that appears to extend to the core-mantle boundary (Nelson and Grand, 2018).

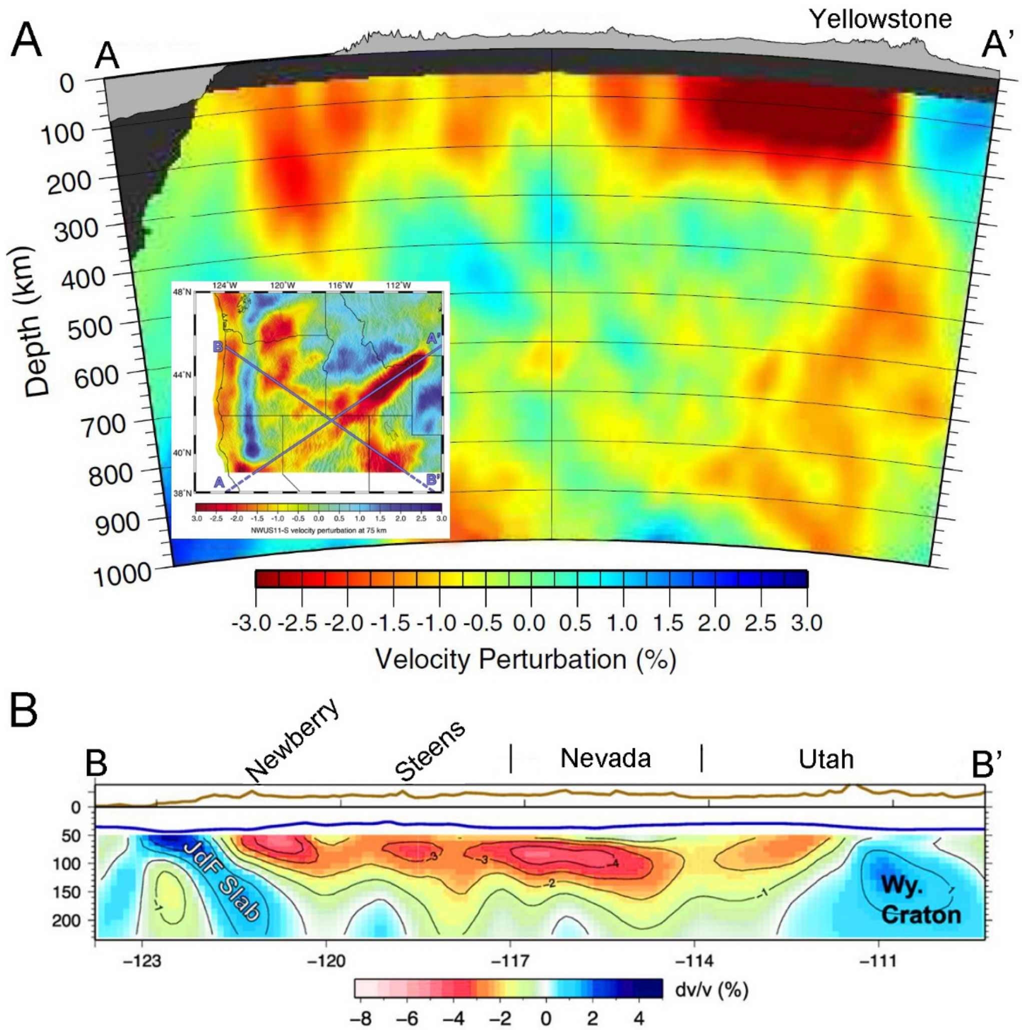

Figure DR2. Cross-sections of low-velocity anomaly. A. S-wave cross-section A-A’ in the direction of plate motion, modified from James et al. (2011). Color saturation +/-3%. Inset showing cross-section locations for A-A’ and B-B’ is map view of S-wave speed perturbations at 75 km depth, modified from Long et al. (2012) using the tomographic model of James et al. (2011). B. S-wave velocity deviations along B-B’, with velocity deviation contours in increments of 1%, modified from Wagner et al. (2010). Brown line is topographic surface; blue line is Moho depth directly above colored velocity deviations.

These similarities provide strong support for long-lived westward flow of plume material emanating from the lower-mantle conduit at least since ~12 Ma, and probably since ~16.5 Ma, with westward-decreasing thermal intensity and chemical fertility of plume-modified mantle resulting from thermomechanical erosion and entrainment of colder, depleted oceanic-type mantle underlying the northern Basin and Range and HLP provinces.

2. Approximation of Yellowstone plume volume flux for source melting, and an estimate of the mantle-flow rate

Hanan et al. (2008) use a mass-balance model of isotopic mixing to show that Snake River Plain tholeiites were little affected by lithospheric pollution and that their isotopic compositions reflect a primary plume source that comprises mass fractions >95% in the derivative lavas. A near constant supply of this fertile source is required to produce a more-or-less steady state in the volume and composition of YSRP basalt over time. Plume volume flux is therefore assumed to keep pace or surpass the pace of plume material being dragged to the SW in the direction of plate motion (Fig. DR3); this assumption was also noted by Schutt and Dueker (2008) in their calculation of buoyancy flux for the Yellowstone plume.

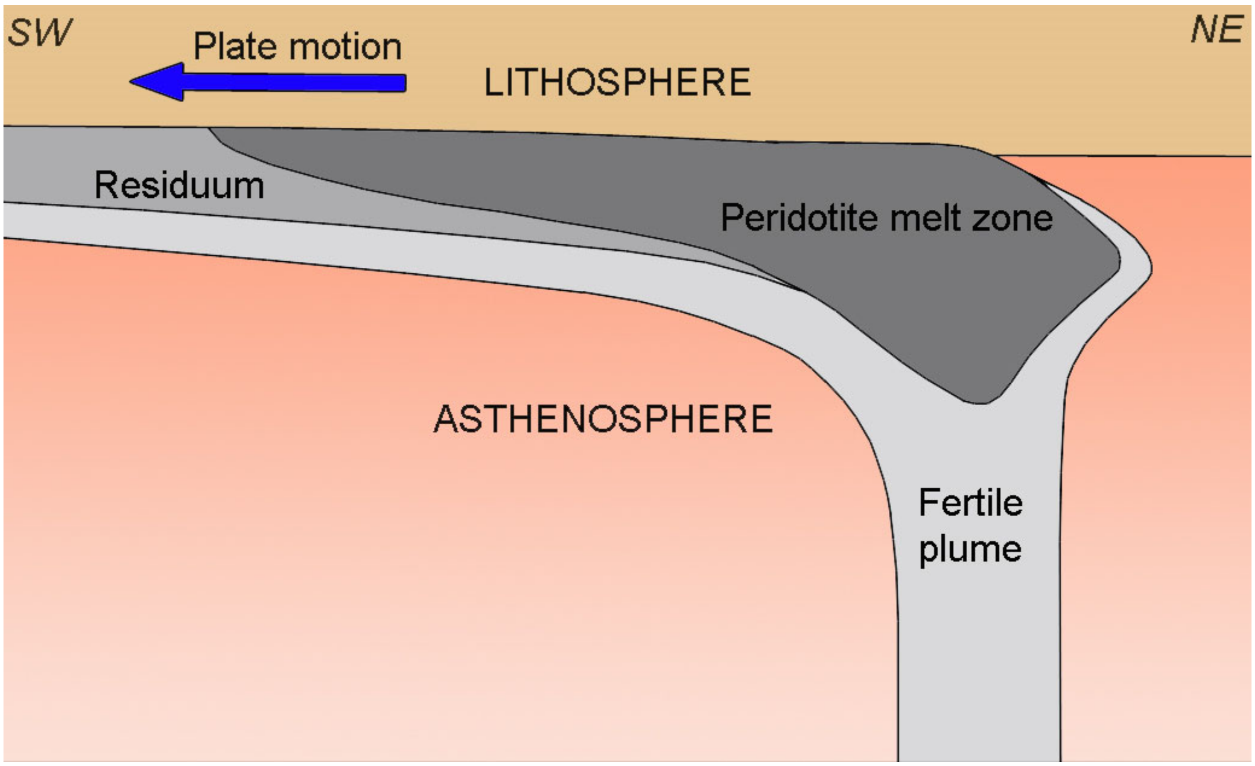

Fig. DR3. Diagrammatic representation of plume-tail melting modified from the descriptions of Wyllie (1988), Ribe and Christensen (1999), and Smith et al. (2009). Rising plume material is dragged to the left, in the direction of asthenospheric flow and plate motion. The melt fraction of fertile lherzolitic peridotite is greatest near the plume axis where temperatures are hotter, leaving a residuum of more refractory harzburgitic peridotite "down wind" of the plume tail.

Volume flux for the basaltic source is estimated here from the rate of mafic melt production and the degree of partial melting. McCurry and Rodgers (2009) use an isotopic mass-balance model to calculate a volume of ~340,000 km^3 of mantle-derived melt that has been added to the YSRP crust between 11 and 4 Ma. This equates to a melt accumulation rate of 48,571 km^3/Ma. Partial melting models using 18 incompatible trace elements indicate that the central Snake River Plain basalts were generated by 5%–10% partial melting (Shervais et al., 2005), similar to the melting range at Kilauea (Piestruszka and Garcia, 1999) and other young tholeiitic basalt provinces (e.g., Herzberg and Gazel, 2009). Melting from 5%–10% at a constant rate of source replacement generates a range in volume flux from 971,420 km^3/Ma to 485,710 km^3/Ma, respectively (or, from 30.78 m^3 s^{-1} to 15.39 m^3 s^{-1}). The total plume flux, however, must also consider the volume flux of fertile mantle beneath the melt zone (Fig. DR3); the latter is unknown but could be significant. The most conservative volume flux value of 15.39 m^3 s^{-1} assumes the highest degree of partial melting (10%) without consideration of the additional flux of plume material beneath the melt zone. Realistically, the actual plume flux is likely to be in somewhere in excess of this minimum value, perhaps exceeding 30 m^3 s^{-1}.

A minimum value for the horizontal mantle-flow rate in the low-velocity channel beneath the YSRP can be estimated by dividing the minimum volume flux (15.39 m^3 s^{-1} = 485,710 km^3/Ma) by the cross-sectional area of the channel. Stachnick et al. (2008) measured the channel cross-section to be 150 km wide and 55 km high at a distance ~250 km SW of the plume conduit. Using rectangular cross-section of these dimensions generates an area of 8250 km^2 which yields an asthenosphere flow rate estimate of ~59 km/Ma. This minimum mantle-flow rate is faster than plate motion (26 km/Ma; Gripp and Gordon, 2002), but similar to the mantle flow rate of 53 km/Ma determined from vector analysis beneath SE Oregon (Ford et al., 2013).

References

Crough, S.T., 1983, Hotspot swells, Annual Reviews Earth and Planetary Science, 11, p. 165-193.

Dodson, A., Kennedy, B.M., and DePaolo, D.J., 1997, Helium and neon isotopes in the Imnaha Basalt, Columbia River Basalt Group: evidence for a Yellowstone plume source: Earth and Planetary Science Letters, v. 150, p. 443-451.

Ford, M.T., Grunder, A.L., Duncan, R.A., 2013, Bimodal volcanism of the High Lava Plains and northwestern Basin and Range of Oregon: distribution and tectonic implications of age-progressive rhyolites: Geochemistry Geophysics Geosystems, v. 14, p. 2836–2857, doi.org/10.1002/ggge.20175

Graham, D.W., Reid, M.R., Jordan, B.T., Grunder, A.L., Leeman, WP., and Lupton, J.E., 2009, Mantle source provinces beneath the northwestern USA delimited by helium isotopes in young basalts: Journal of Volcanology and Geothermal Research, v. 188, doi:10.1016.j.jvolgeores.2008.12.004.

Gripp, A.E., and Gordon, R.G., 2002, Young tracks of hot-spots and current plate velocities, Geophysical Journal International, v. 150, p. 321-361, doi:10.1046/j.1365-246X.2002.0627.x.

Hanan, B.B., Shervais, J.W., and Vetter, S.K., 2008, Yellowstone plume-continental lithosphere interaction beneath the Snake River Plain, Geology, v. 36, p. 51-54, doi:10.1130/G23935A.1.

Herzberg, C., and Gazel, E., 2009, Petrologic evidence for secular cooling in mantle plumes, nature, v. 458, doi: 10.1038/nature 07857.

James, D.E., Fouch, M.J., Carlson, R.W., and Roth, J.B., 2011, Slab fragmentation, edge flow and the origin of the Snake River Plain hotspot track: Earth and Planetary Science Letters, v. 311, p. 124-135, doi:10.1016/j.epsl.2011.09.007.

Leonard, T., and Liu, L., 2016, The role of mantle plume in the formation of Yellowstone volcanism, Geophysical Research Letters, v. 43, doi:10.1002/2015GL067131.

Long, M.D., Till, C.B., Druken, K.A., Carlson, R.W., Wagner, L.S., Fouch, M.J., James, D.E., Grove, T.L., Schmerr, N., Kincaid, C., 2012. Mantle dynamics beneath the Pacific Northwest and the generation of voluminous back-arc volcanism: Geochemistry Geophysics Geosystems. v. 13, doi.org/10.1029/2012gc004189,Q0AN01.

Lowry, A.R., Ribe, N.M., and Smith, R.B., 2000, Dynamic elevation of the Cordillera, western United States: Journal of Geophysical Research, v. 105, p. 23,371-23,390.

McCurry, M., and Rodgers, 2009, Mass transfer along the Yellowstone hot spot track I: Petrologic constraints on the volume of mantle-derived magma, Journal of Volcanology and Geothermal Research, doi:101016/j.jvolgeores.2009.04.001.

Nelson, P.L., and Grand, S.P., 2018, Lower-mantle plume beneath the Yellowstone hotspot revealed by core waves: Nature Geoscience, v. 11, p. 280-284, doi:10.1038s41561-018-0075-y.

Obrebski, M., Allen, R.M., Xue, M., and Hung, S-H., 2010, Slab-plume interaction beneath the Pacific Northwest: Geophysical Research Letters, v. 37, L14305, doi:10.1029/2010GL043489.

Parsons, T., Thompson, G.A., and Sleep, N.H., 1994, Mantle plume influence on the Neogene uplift and extension of the U.S. western Cordillera?, Geology, v. 33, p. 83-86, doi:10.1130/0091-7613(1994)002<0083:MPIOTN>2.3.CO;2.

Pietruszka, A.J., and Garcia, M.O., 1999, A rapid fluctuation in mantle source and melting history of Kilauea Volcano inferred from the geochemistry of its historic summit lavas (1790-1982) , Journal of

Petrology, v. 40, p. 1321-13-42.

Ribe, N.M., and U. Christensen, 1994, Three-dimensional modeling of plume-lithosphere interaction, Journal of Geophysical Research, v. 99, p. 669-682.

Ribe, N.M. and U. Christensen, 1999, The dynamical origin of Hawaiian volcanism, Earth and Planetary Science Letters, v. 171, p. 517-531.

Saltus, R.W., and G.A. Thompson, Why is it downhill from Tonopah to Las Vegas? A case for mantle plume support of the high northern Basin and Range, *Tectonics, 14*, 1235-1244, 1995.

Schutt, D.L., and Dueker, K., 2008, Temperature of the plume layer beneath the Yellowstone hotspot, Geology, v. 36, p. 623-626, doi:10.1130/G24809A.1.

Shervais, J.W., Kauffman, J.D., Gillerman, V.S., Othberg, K.L., Vetter, S.K., Hobson, V.R., Zarnetske, M., Cooke, M.F., Matthew, S.H., and Hanan, B.B., 2005, Basaltic volcanism of the central and western Snake River Plain: A guide to field relations between Twin Falls and Mountain Home, Idaho, in Pederson, J., and Dehler, C.M., eds., Interior Western United States: Geological Society of America Field Guide 6, doi: 10.1130/2005.fld006(02).

Sleep, N.H., 1996, Lateral flow of hot plume material ponded at sublithospheric depths: Journal of Geophysical Research, v. 101, p. 28,065-28,083.

Stachnick, J.C., Dueker, K., Schutt, D.L., and Yuan, H., 2008, Imaging Yellowstone plume-lithosphere interactions from inversion of ballistic and diffusive Rayleigh wave dispersion and crustal thickness data, Geochemistry, Geophysics, Geosystems, doi: 10.1029/2008/GC001992.

Streck, M.J., and Grunder, A.L., 2012, Temporal and crustal effects on differentiation of tholeiite and calcalkaline and ferro-trachytic suites, High Lava Plains, Oregon, USA: Geochemistry, Geophysics, Geosystems, v. 13, doi:10.1029/2012GC004237.

Sun, S-S., and McDonough, W.S., 1989, Chemical and isotopic systematics of oceanic basalts: implications for mantle composition and processes: Geological Society of London, Special Publication 42, p. 313-345.

Taylor, R.N., Thirlwall, M.F., Murton, B.J., Hilton, D.R., Gee, M.A.M., 1997, Isotopic constraints on the influence of the Icelandic plume, Earth and Planetary Science Letters, v. 148, p. 1–8.

Tian, Y., and Zhao, D., 2012, P-wave tomography of the western United States: Insight into the Yellowstone hotspot and Juan de Fuca slab: Physics of the Earth and Planetary Interiors, p. 72-84, doi:10.1016/j.pepi.2012.004.

Wagner, L., Forsyth, D.W., Fouch, M.J., and James, D.E., 2010, Detailed three-dimensional shear wave velocity structure of the northwestern United States from Rayleigh wave tomography: Earth and Planetary Science Letters, v. 299, p. 273-284, doi: 10.1016/j.eps.2010.09.005.

Wyllie, P.J., 1988, Magma genesis plate tectonics and chemical differentiation of the Earth, Reviews in Geophysics, v. 26, p. 370-404.

Wolfe, C.J., Solomon, S.C., Laske, G., Collins, J.A., Detrick, R.S., Orcutt, J.A., Bercovici, D., and Hauri, E.H., 2009, Mantle shear-wave velocity structure beneath the Hawaiian hot spot: Science, v. 326, p. 1388-1390, doi: 10.1126/science.1180165.

Wolff, J.A., Ramos, F.C., Hart, G.L., Patterson, J.D., and Brandon, A.D., 2008, Columbia River flood basalts from a centralized crustal magmatic system: Nature Geoscience, v. 1, doi:10.1038.ngeo124.

Wolff, J.A., and Ramos, F.C., 2013, Source material for the main phase of the Columbia River Basalt Group–Geochemical evidence and implications for magma storage and transport, *in* Reidel, S.P., Camp, V.E., Ross, M.E., Wolff, J.A., Martin, B.S., Tolan, T.L., and Wells, R.E., eds., The Columbia River Flood Basalt Province: Geological Society of America Special Paper 497, doi:10.1130/2013.2497(11).

Zhou, Q., Liu, L., Hu, J., 2018, Western US volcanism due to intruding oceanic mantle driven by ancient Farallon slabs, Nature Geoscience, v. 11, p. 70-76, doi:10.1038/s41516-017-0035-y.